AGU ADVANCING EARTH AND SPACE SCIENCE

Geophysical Research Letters®

RESEARCH LETTER
10.1029/2021GL097250

Changes in the Kuroshio Path, Surface Velocity and Transport During the Last 35,000 Years

Haiyan Yang[1], Xinyu Guo[2,3], Yasumasa Miyazawa[3], Sergey M. Varlamov[3], Ayako Abe-Ouchi[4], and Wing-Le Chan[4]

[1]Graduate School of Science and Engineering, Ehime University, Matsuyama, Japan, [2]Center for Marine Environmental Studies, Ehime University, Matsuyama, Japan, [3]Japan Agency for Marine-Earth Science and Technology, Yokohama, Japan, [4]Atmosphere and Ocean Research Institute, University of Tokyo, Tokyo, Japan

Abstract We consider the sea level, air–sea heat flux, and wind stresses and use an ocean model to investigate the evolution of the Kuroshio path and intensity during the last 35,000 years. Relative to the present, the Kuroshio during the last glacial period traveled the same path albeit with higher surface velocity in the East China Sea, while it migrated northward south of Japan and southward at the Kuroshio Extension (KE). The southward migrations of the KE axis were closely related to the positions of zero wind-stress curl. To a certain extent, stronger glacial trade winds enhanced the North Equatorial Current. Consequently, Kuroshio transport increased in the southern and middle Okinawa Trough. Regarding Kuroshio strength, we suggest that the horizontal gradient of the subsurface temperature would be a better indicator than the upper-ocean vertical thermal gradient, which is a commonly used index in paleoceanography.

Plain Language Summary The last glacial age was characterized by millennial-scale climate variations and sea-level changes. Although the path and intensity of the Kuroshio during the last glacial age have been studied extensively, the evolution of the Kuroshio is still poorly understood because of limited observations and incomplete model configurations. Using an improved ocean model and paleoclimate air–sea forcing field, we simulated the changes in the Kuroshio and Kuroshio Extension (KE) from 35,000 years ago to the present. Compared to the present, the North Pacific subtropical gyre including its southern and northern boundaries (i.e., North Equatorial Current and KE) shifted southward during the glacial age, which was associated with the changes in the wind-stress curl over the North Pacific. The North Equatorial Current and its northern branch (i.e., Kuroshio) was enhanced during the last glacial period. Consequently, the Kuroshio transport increased with a higher surface velocity in the southern and middle East China Sea. With sea level lowering and climatic variations at glacial times, the Kuroshio path south of Japan shifted northward. The KE shifted southward with a range of 0.5–3.5°, which depended on the longitudes. The Kuroshio Current at 6 ka became similar to that of modern day.

Key Points:

- Ocean modeling suggests that, due to an enhanced North Equatorial Current, Kuroshio was stronger during last glacial period than at present
- Southward migration of the Kuroshio Extension during the last glacial period was between 0.5 and 3.5° depending on the longitudes
- Model results indicate that the vertical thermal gradient in the upper ocean is not a suitable indicator of the Kuroshio intensity

Supporting Information:

Supporting Information may be found in the online version of this article.

Correspondence to:

X. Guo,
guoxinyu@sci.ehime-u.ac.jp

Citation:

Yang, H., Guo, X., Miyazawa, Y., Varlamov, S. M., Abe-Ouchi, A., & Chan, W.-L. (2022). Changes in the Kuroshio path, surface velocity and transport during the last 35,000 years. *Geophysical Research Letters*, *49*, e2021GL097250. https://doi.org/10.1029/2021GL097250

Received 29 NOV 2021
Accepted 29 JAN 2022

Author Contributions:

Formal analysis: Haiyan Yang
Supervision: Xinyu Guo
Writing – original draft: Haiyan Yang
Writing – review & editing: Xinyu Guo, Yasumasa Miyazawa, Sergey M. Varlamov, Ayako Abe-Ouchi, Wing-Le Chan

1. Introduction

The Kuroshio Current (KC) is a strong western boundary current in the North Pacific, entering the Okinawa Trough via the Yonaguni Depression off the eastern coast of Taiwan, flowing along the continental slope of the East China Sea (ECS), and eventually turning eastward through the Tokara Strait. After passing the area south of Japan, the Kuroshio separates from the coast of Japan and flows eastward as the Kuroshio Extension (KE) (Figure 1a). The Kuroshio transports warm water from the tropics to the mid-latitudes, and variations in its path and volume transport may influence profoundly the climate in East Asia (Gallagher et al., 2015; S. Kim et al., 2017).

In the last few decades, there has been increasing interest in the Kuroshio variations during the past 40,000 years. The KC in the Last Glacial Maximum (LGM; ~21 ka BP) was initially thought to be deflected to the east into the Pacific because of the land bridge between the Ryukyu Arc and Taiwan (Ahagon et al., 1993; H. Ujiié et al., 1991). However, many proxies in the Okinawa Trough, such as planktonic foraminiferal assemblages, oxygen isotopes, and sediment characteristics, indicated the inflow of the KC into the ECS during the last glacial period (Amano & Itaki, 2016; D. W. Li et al., 2018; Kawahata & Ohshima, 2004; Xu & Oda, 1999). In addition to this pathway, it has been suggested that the KC intrusion into the Okinawa Trough was reduced during the LGM and early deglaciation (D. W. Li et al., 2018; Ijiri et al., 2005; Xiang et al., 2007; Y. Ujiié et al., 2016). However,

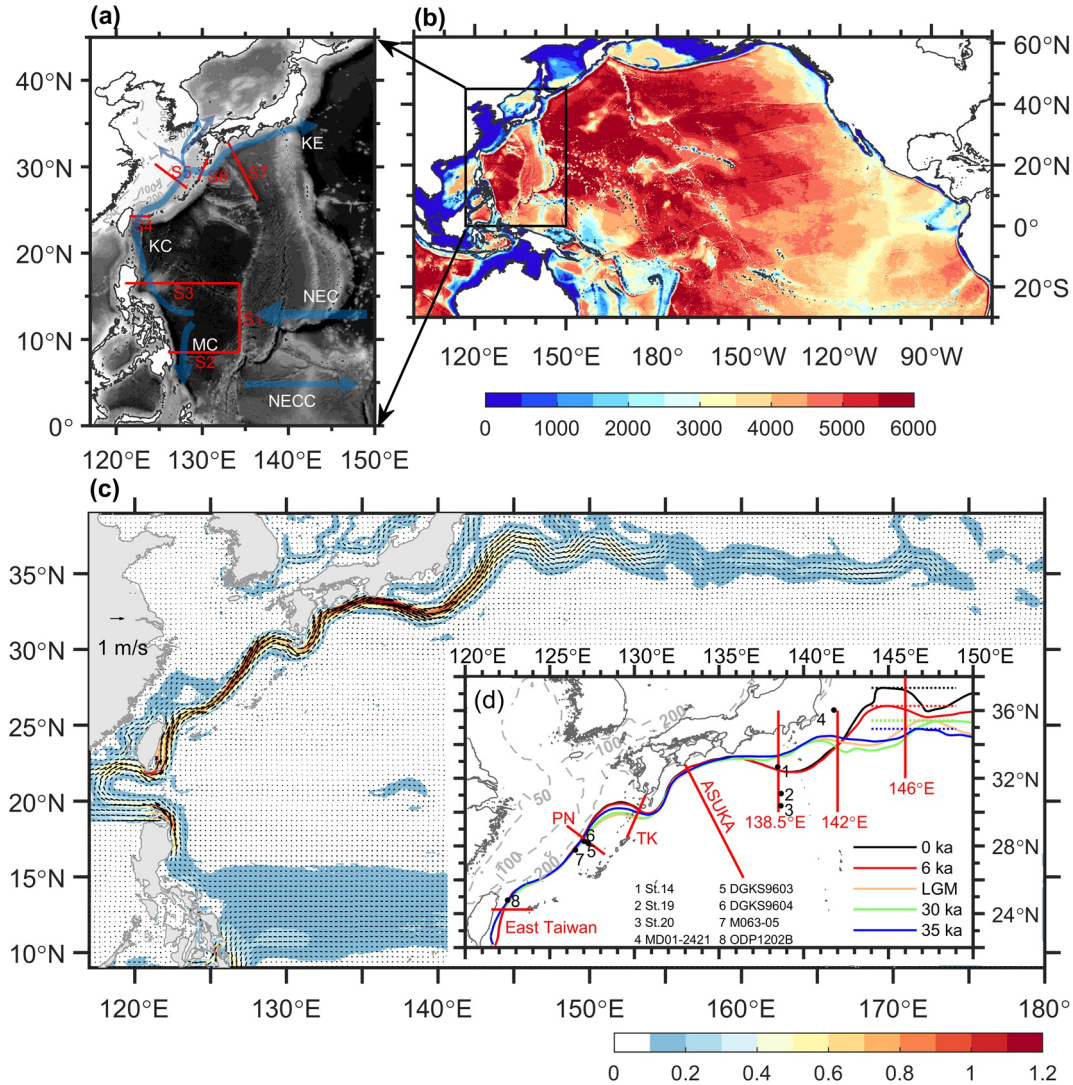

Figure 1. (a) Northwest Pacific Ocean bathymetry (shaded colors; unit: m) and ocean circulation (semitransparent blue arrows) map. Red lines indicate sections used for volume transports in Table S2 in Supporting Information S1. The NEC, NECC, MC, Kuroshio Current (KC), and Kuroshio Extension (KE) acronyms stand for North Equatorial Current, North Equatorial Countercurrent, Mindanao Current, KC, and KE, respectively. (b) Domain and bathymetry of the model. Colors indicate model bathymetry (unit: m). (c) Annual mean surface current (0–100 m, unit: m/s) in the Northwest Pacific. Shading indicates the area where current speed exceeds 0.1 m/s. (d) Kuroshio axes in five different experiments. Gray dotted lines indicate the East China Sea depths; other dotted lines indicate the northern KE limits. Red lines indicate sections for checking the velocity cores and water temperatures. Black circles (from 1 to 8) are the sediment cores used in our discussion.

based on the temperature and nutrient conditions, the Kuroshio transport could be stronger (Kubota et al., 2017). Thus far, it remains unclear whether the paleo-KC was stronger or weaker.

The KE is at the northern boundary of the North Pacific subtropical gyre. Early studies of planktic foraminiferal assemblages reported that the boundary region of the subtropical-subarctic gyre and the KE shifted southward during the last glacial period (Gallagher et al., 2015; Harada et al., 2004; Kawahata & Ohshima, 2002; Seo et al., 2018; Thompson, 1981; Thompson & Shackleton, 1980; Yamamoto, 2009). However, Sawada and Handa (1998) suggested northward Kuroshio migrations off the coast of Central Japan from 26 to 24.5 and 21 to 19 ka BP. To date, the paleo-KC path and intensity have been investigated and debated, but observations have very limited spatial and temporal scales.

In addition to these observations, ocean models have significantly improved our paleo-KC understanding. Earlier models have shown that the KC entered the Okinawa Trough with a stronger surface current and a reduced volume transport during the LGM (Kao et al., 2006; Lee et al., 2013; Vogt-Vincent & Mitarai, 2020; Zheng et al., 2016), but the mechanism was not adequately explained. Most modeling studies considered only the effect of sea-level lowering on the KC, using low-resolution models that were unable to resolve mesoscale eddies adequately. Moreover, earlier regional models, which relied greatly on the specified boundary conditions, focused on the ECS but excluded the KE system. It was indicated that the westerly jet stream over the North Pacific during the LGM migrated southward compared to the present position (Gray et al., 2020; N. Wang et al., 2018; Yanase & Abe-Ouchi, 2010). However, few of the existing modeling studies explicitly explored the relative extent and strength of the paleo-KE under the combined influences of sea level and climate. A large-scale ocean model for studying the Kuroshio region including the KE system is therefore necessary.

For the Kuroshio and its adjacent regions, the condition of the KC is affected by millennial-scale changes in the atmosphere and equatorial Pacific (Y. Ujiié et al., 2016). The KE dynamics are influenced by wind forcing over the mid-latitude North Pacific, and the KE variability is mainly due to westward propagating mesoscale eddies from the central and eastern North Pacific (Qiu, 2003, 2014; Sasaki & Schneider, 2011). Here, our ocean model configuration considers the climatic (i.e., air–sea heat flux and wind stresses) and sea-level changes over the entire North Pacific. We simulate how the KC responded to the combined changes during five historical ages (0 (i.e., present), 6, 21 (i.e., LGM), 30, and 35 ka BP), particularly in terms of the Kuroshio path, surface velocity, and transport. Using the simulated water-temperature data, we assess whether the vertical temperature gradient is a reliable KC intensity indicator.

2. Materials and Methods

The ocean model is the Stony Brook Parallel Ocean Model (sbPOM), and the model domain covers the entire North Pacific and part of the South Pacific (30°S–62°N, 100°E−90°W), with a horizontal resolution of 1/12° and 47 sigma levels in the vertical direction (Figure 1b in Supporting Information S1). Based on the global mean sea level given by Yokoyama et al. (2018) for the past 35 ka, the reductions in water depth due to lowering of sea level in four experiments from 35 ka to 6 ka were decided (Table S1 in Supporting Information S1). Among these experiments, the Tsushima Strait is closed at LGM (Figure S1 in Supporting Information S1).

The meteorological and oceanic data used for the four paleo-experiments were provided by the fully coupled atmosphere–ocean general circulation model MIROC4m (Chan et al., 2011; in Supporting Information S1). To reduce the potential impact of model bias on our model results, we modified the MIROC4m paleo-data (i.e., air–sea heat flux and wind stresses) with the standard 0 ka BP data (in Supporting Information S1).

We compared the air–sea heat flux differences between the paleo-ages and 0 ka BP (Figure S2 in Supporting Information S1) and checked the zero wind-stress curl positions (Figure S3 in Supporting Information S1). In the glacial ages (LGM, 30, and 35 ka BP), the ocean lost more heat (>20 W/m^2) to the atmosphere in the Kuroshio region, whose cooling effect has been indicated from the variations in subtropical SSTs (Sagawa et al., 2011). Meanwhile, the westerly jet stream shifted southward by ∼1.0° in the North Pacific.

3. Results

3.1. Kuroshio Path

The annual mean Kuroshio axis for the five ages is defined by the maximum velocity along the Kuroshio (Figures 1d and Ambe et al., 2004). Compared to the modern KC, the KC at 6 ka BP exhibits almost the same position east of Taiwan (Figure S6a in Supporting Information S1), along the ECS shelf slope and south of Japan. However, the glacial KC axes east of Taiwan shift shoreward compared to the modern KC (Figure S6a in Supporting Information S1). The location of the KC axis at the PN section has no migration at 35 ka BP but shifts seaward during the LGM and at 30 ka BP (Figure S7a in Supporting Information S1). The glacial KC tends to shift seaward in the Tokara Strait (Figure S6b in Supporting Information S1). In addition, the seaward shift distance is likely proportional to the lowered sea level because the KC axis exhibits the southernmost displacement during the LGM when the sea level is the lowest.

The Kuroshio path south of Japan (i.e., 131.0–136.5°E) is very similar among the five cases (Figure 1c), especially in the region south of Shikoku (e.g., the ASUKA section; Figure S8 in Supporting Information S1). However, the glacial KC axes southeast of Japan (i.e., 136.5–142.0°E) migrate northward (Figure S9 in Supporting Information S1), and present the largest migration of ∼1.5° at 140°E. The KE migrates northward at 142°E at 6 ka BP, LGM, and 35 ka BP (Figure S10 in Supporting Information S1), and southward at 146°E (Figure S7b in Supporting Information S1) for 1.0 and 2.0° ranges in 6 ka BP and glacial ages, respectively. In the KE region (i.e., 142–150°E). By comparison, the southward migration of the glacial KE axes range from 0.5 to 3.5° at different longitudes. Compared to the latitudinal KE amplitude at 0 ka BP, the paleo-KE axes meander with smaller amplitudes, and the smallest meandering amplitude occurs at 35 ka BP.

3.2. Kuroshio Surface Velocity

In the area east of Taiwan, there is little difference in the KC surface velocity between 6 and 0 ka BP. The glacial KC surface velocities, whose maximum values are located closer to the shore (Figure S6a in Supporting Information S1), are stronger. In the central ECS (PN section in Figure S7a in Supporting Information S1), the KC surface current also shows the following two regimes: A weak one (i.e., ∼0.9 m/s) at 0 and 6 ka BP and a strong one (i.e., ∼1.4 m/s) in the glacial ages. As the KC exits the ECS from the Tokara Strait, the glacial KC surface current is still stronger than the modern one (Figure S6b in Supporting Information S1). The KE current speed at the 146°E section (Figure S7b in Supporting Information S1) exceeds 0.4 m/s at 0 ka BP, reduces by ∼0.2 m/s at 6 ka BP and by ∼0.1 m/s at 30 and 35 ka BP; however, it increases by ∼0.1 m/s during the LGM.

3.3. Kuroshio Transport

Based on the annual mean current, the upper 1000 m integrated volume transport stream function was calculated as $\Psi(x, y) = \int_{x_E}^{x} \int_{-1000\ m}^{0} v(x, y, z) dz dx$, where Ψ is the stream function, x_E denotes the eastern boundary of the Pacific, and v (x, y, z) is the northward velocity at the point with x, y, and z (i.e., longitude, latitude, and depth, respectively) coordinates. In Figure 2, contours at 0 and 6 ka BP have similar distributions and values. As the 20 and 30 Sv contours show, the KC transports into the continental shelf break northeast of Taiwan. In the region southeast of Kyushu, the KC merges with the Ryukyu Current, so the Kuroshio volume transport is significantly increased after exiting the ECS through the Tokara Strait. In the region south of Japan, anticyclonic recirculation exists all the time and contributes to the Ryukyu Current. Compared to the stream-function contours at 0 ka BP, the southern boundary of the subtropical gyre in the glacial ages is located further south. In addition, there is a larger amount of water transported by the NEC to mid-latitude regions in the glacial ages, indicating stronger subtropical gyres in the glacial ages compared to those at 0 and 6 ka BP.

We calculated the mean volume transports in the upper 1,000 m at seven sections (i.e., S1–S7 in Supporting Information S1; Figure 1a) across the main currents in the northwest Pacific (Table S2 in Supporting Information S1). The volume transport values at 0 ka BP are comparable to the observed values, and they appear to be very similar to the values at 6 ka BP. However, the NEC (i.e., the origin of the Kuroshio) exhibits the following large significant increases in westward volume transports: 16.4, 17.1 and 13.6 Sv at LGM, 30 and 35 ka BP, respectively. This is also evident in the volume-transport stream function (Figure 2). Based on the values at S1 to S3 (Table S2 in Supporting Information S1), the Kuroshio bifurcates from the NEC, thereby further increasing the northward volume transports, which are 13.4, 14.0, and 9.3 Sv at the LGM, 30 and 35 ka BP, respectively, all of which are greater than the 0 ka BP volume transport. Conversely, the glacial Mindanao Current exhibits slightly decreased volume transport. Therefore, in the glacial ages, most of the increased NEC transport is supplied to the KC.

The Kuroshio flows northward along the east Philippine coast, and then exchanges water with the South China Sea through the Luzon Strait. The 0 ka BP volume transport in the upper 1,000 m across the Luzon Strait is westward and eastward at 25.1 and 18.5 Sv, respectively. Net volume transports are westward and amount to 6.6, 6.0, 1.4, 1.9, and 3.8 Sv at 0, 6 ka BP, LGM, 30 and 35 ka BP, respectively. The KC east of Taiwan is separated into two branches, one of which enters the ECS as the Kuroshio mainstream, and the other flows eastward along the south edge of the Ryukyu Islands. The volume transports of both branches in the glacial ages are ∼4.0 Sv larger than those at 0 ka BP. In the ECS, the KC outflow through the Kerama Gap forms an anticyclonic recirculation in the region southeast of the Kerama Gap, while its volume transport increases by ∼2.0 Sv in glacial ages compared to 0 ka BP. Meanwhile, there is a slight increase by ∼1.1 Sv in the glacial Kuroshio transport at the PN section.

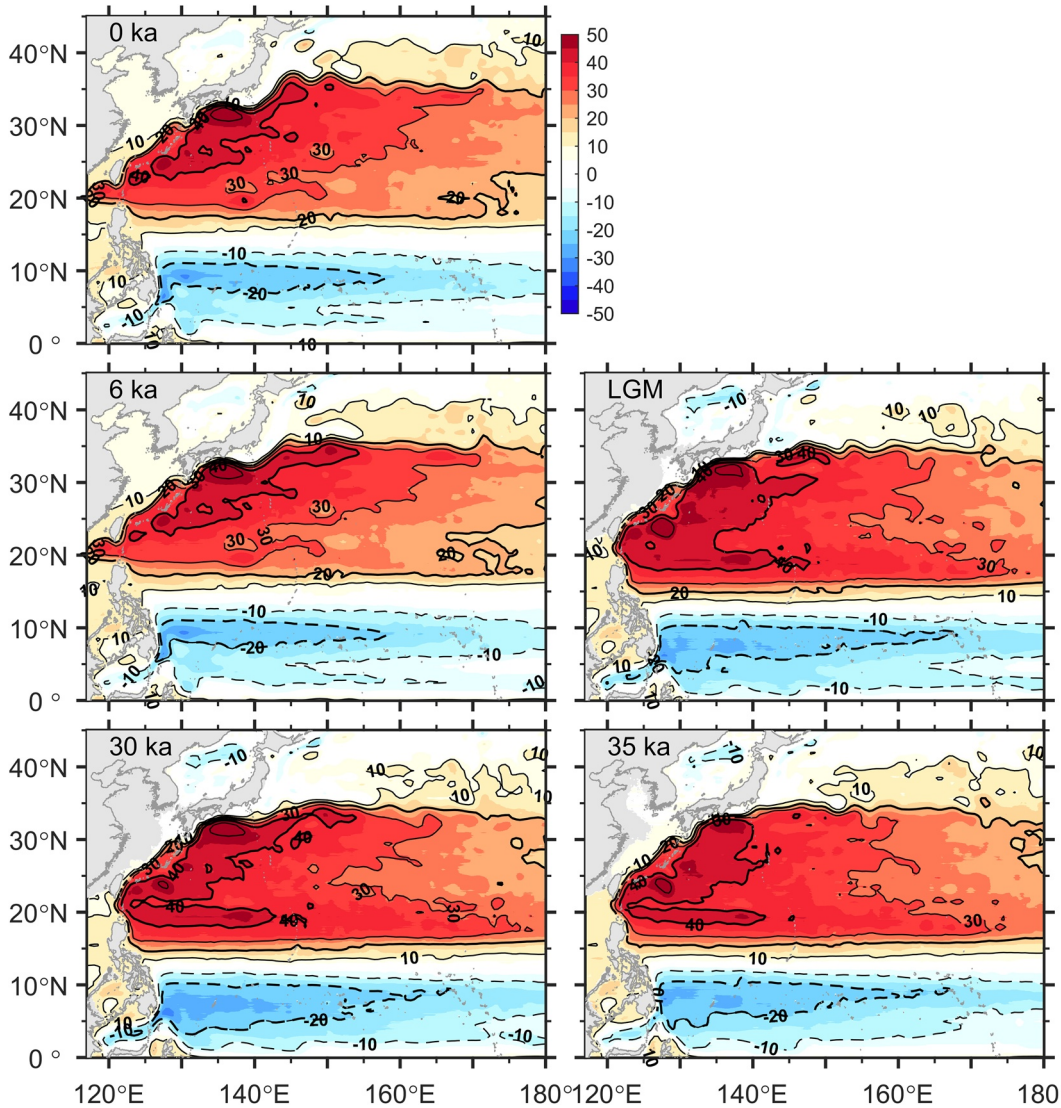

Figure 2. Upper 1000 m integrated volume-transport stream function (unit: Sv; 1 Sv = 10^6 m^3/s) in the 5 ages.

Eventually, the KC in the ECS and the Ryukyu Current merge and form the KC south of Japan. The net volume transport increases to 31.6 Sv (i.e., 0 ka BP) at section ASUKA. The volume transports there reach 39.2, 36.8, and 34.1 at the LGM, 30 and 35 ka BP, respectively; such increased meridional transports are evident also in Figure 2.

4. Discussion

4.1. Kuroshio Path, Surface Velocity, and Transport

Compared to the present location of the KC in the ECS, the KC axes shift slightly seaward at the LGM and 30 ka BP (Figure S7a in Supporting Information S1). Such southeastward shift has also been reported by another ocean model study (Vogt-Vincent & Mitarai, 2020) and a sediment core study (Kubota et al., 2017).

Up to now, a limited number of cores (i.e., stations 14, 19, 20 and MD01-2421; Figure 1d) suggested that the KC off the coast of central Japan and KE moved northward during the last glacial period (Sawada & Handa, 1998; Yamamoto, 2009) and the KE in the Central Pacific exhibited a southward shift (Kawahata & Ohshima, 2002). In our study, the KC axes southeast of Japan (136.5–142.0°E) migrate northward by about 0.8° at 138.5°E during the glacial ages. The northern limit of the KE axis at 6 ka BP, LGM, 30 and 35 ka BP exhibits southward migration of 1.1, 1.9, 2.0, and 2.4°, respectively. Similarly, the zonal mean wind-stress curl (Figure S3 in Supporting

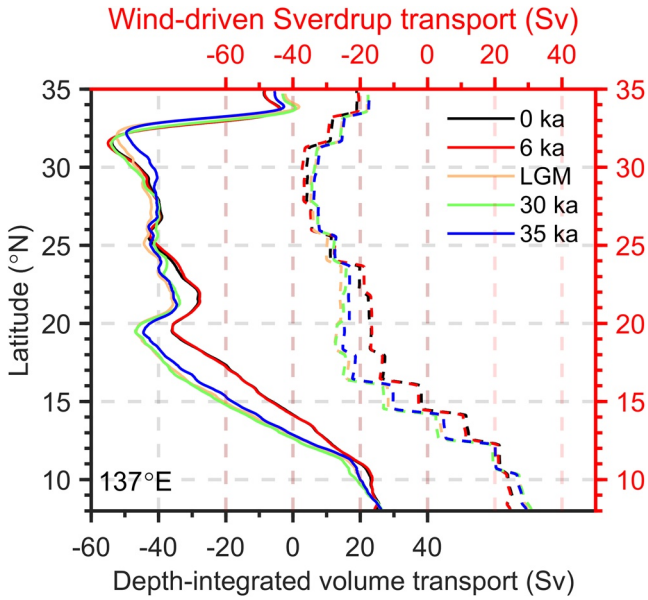

Figure 3. Zonally integrated values in Sv from the east coast to 137°E of modeled volume transport in the upper 1,000 m (solid lines, with reference to the black axes) and wind-driven Sverdrup transport from the east coast to 137°E (dashed lines, with reference to the red axes). All the values are processed with 0.25° running average.

Information S1) reveals that the zero wind-stress curl at 0 ka BP is located at 41.2°N, and it migrates southward by 0.2, 1.1, 0.9, and 1.1° at 6 ka BP, LGM, 30 and 35 ka BP, respectively. Therefore, the southward migrations of the KE axes are likely closely related to the zero wind-stress curl positions. Different latitudinal displacements of the KE should change the distribution of the glacial sea surface temperature, which will be reported elsewhere. We note that the KC path south of Japan depends more on the local topography and upstream conditions, rather than the position of the zero wind-stress curl.

As the wind fields (Figure S3 in Supporting Information S1) shift southward in the glacial ages, the NEC and KE latitudes exhibit southward displacements, indicating a southward shift of the North Pacific subtropical gyre. A more southerly position of the NEC bifurcation results in stronger Kuroshio transport (Hu et al., 2015; Y. L. Wang & Wu, 2018; Weiss et al., 2021). In our simulations, the glacial Kuroshio transport in the southern and middle Okinawa Trough increases with a higher surface velocity, which is due to the stronger NEC, as shown in Section 3.3. Compared to the present, the Kuroshio intrusion into the northern Okinawa Trough is reduced with a weaker current speed in the glacial ages, which is consistent with reconstructed results (Chang et al., 2008; D. W. Li et al., 2018; Ijiri et al., 2005; Shi et al., 2014; Vats et al., 2020). The Tsushima Strait is closed at the LGM and narrow at 30 and 35 ka BP, leading to a decrease in the transport through the Tsushima Strait. Moreover, the KC axis exhibits a southward displacement in the northern Okinawa Trough, which also reduces the northward Kuroshio transport separation.

To quantify the subtropical circulation changes in 5 ages, we zonally integrated the volume transport from the east coast to 137°E for the annual mean transport stream function at different latitudes (solid lines in Figure 3). At 0 and 6 ka BP, the meridional transport is northward south of 14°N, 0 at 14°N, and southward north of 14°N. In the 3 glacial ages, the meridional transport was 0 at 13°N, while exhibiting a southward shift (Figure 3), with values increasing by approximately 10 Sv from 13 to 25°N and indicating a stronger subtropical gyre. Previous sediment cores and an ensemble of general circulation models suggested a stronger North Pacific subtropical gyre during the LGM (Gray et al., 2020; Sawada & Handa, 1998). Therefore, the North Pacific subtropical gyre tends to be stronger and shifts southward in glacial ages.

We also calculated the corresponding wind-driven Sverdrup transport from the east coast to 137°E (dashed lines in Figure S3 in Supporting Information S1). The enhanced North Pacific subtropical gyre in the glacial ages can be partly explained by the stronger wind-stress curl and trade winds (Figure S3 in Supporting Information S1). From 13 to 25°N, the wind-driven Sverdrup transport agrees with gyre strengthening in the glacial ages. However, the Sverdrup transport north of 25°N is weaker in the glacial ages than at 0 and 6 ka BP, which is not consistent with gyre strengthening (Figure 3). Hogg and Gayen (2020) suggested that surface buoyancy fluxes (i.e., mainly heating and cooling in the ocean surface) are essential for the ocean-gyre transport. A significant amount of cooling (Figure S2 in Supporting Information S1) is evident over the Kuroshio region during the glacial ages in our model forcing. Therefore, it is possible that the circulation north of 25°N is driven by the buoyancy forcing rather than the wind stresses.

4.2. A Kuroshio Intensity Indicator

The KC intensity strongly affects the Okinawa Trough water temperatures. Using reconstructed Okinawa Trough water temperatures, many studies have examined the Kuroshio intensity variation since the LGM. The $U^{K'}_{37}$ proxy is usually used as an annual mean SST index (R. A. Kim et al., 2015) and the TEX_{86} proxy most likely reflects subsurface (i.e., <200 m) water temperature (D. Li et al., 2013; Ruan et al., 2017; Zhao et al., 2015). These studies considered that a weaker KC leads to a shallow mixed layer and smaller vertical thermal gradient. The vertical thermal gradient can be estimated from the difference between $U^{K'}_{37}$ and TEX_{86} derived temperature, that

Table 1
Modeled Sea Surface Temperature (SST), Subsurface Temperature (SubST), Their Difference (i.e., ΔT = SST – SubST; Unit: °C), and Surface Velocity (Unit: m/s) at the ODP1202B and M063-05 Sediment Cores

	ODP1202B				M063-05			
Time	SST (0–30 m)	SubST (30–80 m)	Velocity (0–80 m)	ΔT	SST (0–30 m)	SubST (30–200 m)	Velocity (0–200 m)	ΔT
0 ka	25.95	23.01	0.58	2.93	24.91	19.78	0.67	5.14
6 ka	25.79	22.85	0.59	2.94	24.74	19.62	0.66	5.11
LGM	22.67	19.27	1.10	3.40	23.06	16.44	1.20	6.61
30 ka	23.04	19.21	1.04	3.83	23.84	16.91	1.24	6.93
35 ka	23.68	19.82	1.34	3.86	23.68	17.15	1.16	6.52

Note. The depth of SubST at the ODP1202B core is from Ruan et al. (2017) while that at the M063-05 core is from Li et al. (2020).

is, $\Delta T = SST_{U^{K'}_{37}} - SubST_{TEX_{86}}$; hence, ΔT has been used as an indicator of the KC intensity and evolution (Li et al., 2020; Ruan et al., 2017).

The surface thermal buoyancy flux and local wind speed also affect the depth of the thermocline or the surface mixed layer (L. Wang et al., 2016). To confirm the relationship between ΔT and KC intensity, we compared the modeled annual mean ΔT and the modeled surface-current speeds at the two core sites (Table 1). According to Table 1, a stronger KC appears to correspond with a higher ΔT but not a lower ΔT.

The idea that a stronger KC results in a lower ΔT value is not compatible with ocean dynamics. According to the thermal wind relation, the vertical geostrophic-flow variation is proportional to the horizontal water-temperature gradient; a larger horizontal temperature gradient corresponds to a stronger KC. As we described earlier, the SST in the Kuroshio region is affected not only by the Kuroshio speed, but also by the air–sea heat flux and local wind forcing. Consequently, the subsurface water temperature, rather than the SST, is sensitive to the Kuroshio intensity variations (Kubota et al., 2017).

We hypothesized that the subsurface horizontal thermal gradient across the KC is more appropriate as a KC intensity index than the vertical thermal gradient. To confirm this idea, we calculated the difference between the modeled subsurface (i.e., 200 m) water temperature (i.e., $\Delta T_H = SubST_{DGKS9603} – SubST_{DGKS9604}$) between the DGKS9604 and DGKS9603 cores (Figure 1d). The ΔT_H values are 0.49, 0.50, 2.39, 2.00, and 1.49°C at 0, 6 ka BP, LGM, 30 and 35 ka BP, respectively. The maximum current speeds in the upper 200 (500) m are 0.92 (0.07), 0.93 (0.07), 1.47 (0.19), 1.44 (0.17), and 1.40 (0.13) m/s at 0, 6 ka BP, LGM, 30 and 35 ka BP, respectively. There was a significant correlation between ΔT_H and KC speeds; therefore, it is practical to evaluate the KC surface strength by using the horizontal subsurface temperature gradient across the KC. If it is difficult to find two core stations at the direction normal to the Kuroshio axis, the subsurface temperature gradient at the longitudinal or latitudinal direction is also a good index for the KC intensity with the condition that a core station is on both sides of the KC.

5. Conclusions

Considering the changes in sea level, air–sea heat flux, and wind stresses, our model results provide the evolution of the Kuroshio path, transport, and strength from 35 ka BP to the present. The subtropical gyre in the last glacial period becomes stronger and migrates southward, which is related to the wind-stress curl in the North Pacific. The 6 ka BP KC has basically the same path, transport, and strength as the modern KC. It has been confirmed that, the glacial Kuroshio transport increases and KC axis migrates slightly seaward in the ECS. The glacial KC appears to shift southward when it exits the ECS through the Tokara Strait, and exhibits the southernmost shift during the LGM. Moreover, the glacial KC off the southeastern coast of Japan migrates northward with a small meander. The southward migration of the glacial KE varies between 0.5 and 3.5°.

In search for an appropriate KC intensity indicator, we found that the upper-ocean vertical thermal gradient used in some studies is unsatisfactory; therefore, we suggest that it is better to evaluate the KC surface strength using

the horizontal subsurface-temperature gradient across the KC. This conclusion can facilitate future studies on the Kuroshio path and strength variations.

Data Availability Statement

Major simulated data are available at https://doi.org/10.5281/zenodo.5733861.

Acknowledgments
This work was supported by JSPS KAKENHI Grant No. 17H02959, 17H06104, and 17H06323. H. Yang thanks the China Scholarship Council (CSC) for supporting her stay in Japan.

References

Ahagon, N., Tanaka, Y., & Ujiié, H. (1993). Florisphaera profunda, a possible nannoplankton indicator of late Quaternary changes in sea-water turbidity at the northwestern margin of the Pacific. *Marine Micropaleontology*, *22*(3), 255–273. https://doi.org/10.1016/0377-8398(93)90047-2

Amano, A., & Itaki, T. (2016). Variations in sedimentary environments in the forearc and backarc regions of the Ryukyu Arc since 25 ka based on CNS analysis of sediment cores. *Quaternary International*, *397*, 360–372. https://doi.org/10.1016/j.quaint.2015.06.017

Ambe, D., Imawaki, S., Uchida, H., & Ichikawa, K. (2004). Estimating the Kuroshio Axis south of Japan using combination of satellite Altimetry and drifting buoys. *Journal of Oceanography*, *60*(2), 375–382. https://doi.org/10.1023/B:JOCE.0000038343.31468.fe

Chang, Y.-P., Wang, W.-L., Yokoyama, Y., Matsuzaki, H., Kawahata, H., & Chen, M.-T. (2008). Millennial-scale planktic foraminifer faunal variability in the East China Sea during the past 40000 Years (IMAGES MD012404 from the Okinawa Trough). *Terrestrial, Atmospheric and Oceanic Sciences*, *19*(4). https://doi.org/10.3319/TAO.2008.19.4.389(IMAGES)

Gallagher, S. J., Kitamura, A., Iryu, Y., Itaki, T., Koizumi, I., & Hoiles, P. W. (2015). The Pliocene to recent history of the Kuroshio and Tsushima currents: A multi-proxy approach. *Progress in Earth and Planetary Science*, *2*(1), 17. https://doi.org/10.1186/s40645-015-0045-6

Gray, W. R., Wills, R. C. J., Rae, J. W. B., Burke, A., Ivanovic, R. F., Roberts, W. H. G., et al. (2020). Wind-driven evolution of the North Pacific Subpolar Gyre over the last deglaciation. *Geophysical Research Letters*, *47*(6). https://doi.org/10.1029/2019GL086328

Harada, N., Ahagon, N., Uchida, M., & Murayama, M. (2004). Northward and southward migrations of frontal zones during the past 40 kyr in the Kuroshio-Oyashio transition area. *Geochemistry, Geophysics, Geosystems*, *5*(9). https://doi.org/10.1029/2004GC000740

Hogg, A. McC., & Gayen, B. (2020). Ocean Gyres Driven by Surface Buoyancy Forcing. *Geophysical Research Letters*, *47*(16). https://doi.org/10.1029/2020GL088539

Hu, D., Wu, L., Cai, W., Gupta, A. S., Ganachaud, A., Qiu, B., et al. (2015). Pacific western boundary currents and their roles in climate. *Nature*, *522*(7556), 299–308. https://doi.org/10.1038/nature14504

Ijiri, A., Wang, L., Oba, T., Kawahata, H., Huang, C.-Y., & Huang, C.-Y. (2005). Paleoenvironmental changes in the northern area of the East China Sea during the past 42,000 years. *Palaeogeography, Palaeoclimatology, Palaeoecology*, *219*(3–4), 239–261. https://doi.org/10.1016/j.palaeo.2004.12.028

Kao, S. J., Wu, C.-R., Hsin, Y.-C., & Dai, M. (2006). Effects of sea level change on the upstream Kuroshio Current through the Okinawa Trough. *Geophysical Research Letters*, *33*(16). https://doi.org/10.1029/2006GL026822

Kawahata, H., & Ohshima, H. (2002). Small latitudinal shift in the Kuroshio Extension (Central Pacific) during glacial times: Evidence from pollen transport. *Quaternary Science Reviews*, *21*(14–15), 1705–1717. https://doi.org/10.1016/S0277-3791(01)00150-0

Kawahata, H., & Ohshima, H. (2004). Vegetation and environmental record in the northern East China Sea during the late Pleistocene. *Global and Planetary Change*, *41*(3–4), 251–273. https://doi.org/10.1016/j.gloplacha.2004.01.011

Kim, R. A., Lee, K. E., & Bae, S. W. (2015). Sea surface temperature proxies (alkenones, foraminiferal Mg/Ca, and planktonic foraminiferal assemblage) and their implications in the Okinawa Trough. *Progress in Earth and Planetary Science*, *2*(1), 43. https://doi.org/10.1186/s40645-015-0074-1

Kim, S., Son, H.-Y., & Kug, J.-S. (2017). How well do climate models simulate atmospheric teleconnctions over the North Pacific and East Asia associated with ENSO? *Climate Dynamics*, *48*(3–4), 971–985. https://doi.org/10.1007/s00382-016-3121-8

Kubota, Y., Suzuki, N., Kimoto, K., Uchida, M., Itaki, T., Ikehara, K., et al. (2017). Variation in subsurface water temperature and its link to the Kuroshio Current in the Okinawa Trough during the last 38.5 kyr. *Quaternary International*, *452*, 1–11. https://doi.org/10.1016/j.quaint.2017.06.021

Lee, K. E., Lee, H. J., Park, J.-H., Chang, Y.-P., Ikehara, K., Itaki, T., & Kwon, H. K. (2013). Stability of the Kuroshio path with respect to glacial sea level lowering. *Geophysical Research Letters*, *40*(2), 392–396. https://doi.org/10.1012/grl.50102

Li, D., Zhao, M., Tian, J., & Li, L. (2013). Comparison and implication of TEX^{H}_{86} and $U^{K'}_{37}$ temperature records over the last 356 kyr of ODP Site 1147 from the northern South China Sea. *Palaeogeography, Palaeoclimatology, Palaeoecology*, *376*, 213–223. https://doi.org/10.1016/j.palaeo.2013.02.031

Li, D.-W., Chang, Y.-P., Li, Q., Zheng, L., Ding, X., & Kao, S.-J. (2018). Effect of sea-level on organic carbon preservation in the Okinawa Trough over the last 91 kyr. *Marine Geology*, *399*, 148–157. https://doi.org/10.1016/j.margeo.2018.02.013

Li, Q., Li, G., Chen, M., Xu, J., Liu, S., & Chen, M. (2020). New insights into Kuroshio Current evolution since the last deglaciation based on paired organic paleothermometers from the middle Okinawa Trough. *Paleoceanography and Paleoclimatology*, *35*(12). https://doi.org/10.1029/2020PA004140

Qiu, B. (2003). Kuroshio extension variability and forcing of the Pacific decadal oscillations: Responses and potential Feedback. *Journal of Physical Oceanography*, *33*(12), 2465–2482. https://doi.org/10.1175/2459.1

Qiu, B., Chen, S., Schneider, N., & Taguchi, B. (2014). A coupled decadal Prediction of the dynamic state of the Kuroshio extension system. *Journal of Climate*, *27*(4), 1751–1764. https://doi.org/10.1175/JCLI-D-13-00318.1

Ruan, J., Xu, Y., Ding, S., Wang, Y., & Zhang, X. (2017). A biomarker record of temperature and phytoplankton community structure in the Okinawa Trough since the last glacial maximum. *Quaternary Research*, *88*(1), 89–97. https://doi.org/10.1017/qua.2017.28

Sagawa, T., Yokoyama, Y., Ikehara, M., & Kuwae, M. (2011). Vertical thermal structure history in the western subtropical North Pacific since the last glacial maximum. *Geophysical Research Letters*, *38*(8). https://doi.org/10.1029/2010GL045827

Saito, H., Suzuki, K., Takahashi, M., & Nagai, T. (2019). *Kuroshio current physical, biogeochemical, and ecosystem dynamics*. Retrieved from https://onlinelibrary.wiley.com/doi/book/10.1002/9781119428428

Sasaki, Y. N., & Schneider, N. (2011). Decadal shifts of the Kuroshio Extension jet: Application of thin-jet theory*. *Journal of Physical Oceanography*, *41*(5), 979–993. https://doi.org/10.1175/2011JPO4550.1

Sawada, K., & Handa, N. (1998). Variability of the path of the Kuroshio Ocean current over the past 25,000 years. *Nature*, *392*(6676), 592–595. https://doi.org/10.1038/33391

Seo, I., Lee, Y., Yoo, C. M., & Hyeong, K. (2018). Migration of the Kuroshio Extension in the northwest Pacific since the last glacial maximum. *Palaeogeography, Palaeoclimatology, Palaeoecology*, *496*, 323–331. https://doi.org/10.1016/j.palaeo.2018.01.048

Shi, X., Wu, Y., Zou, J., Liu, Y., Ge, S., Zhao, M., et al. (2014). Multiproxy reconstruction for Kuroshio responses to northern hemispheric oceanic climate and the Asian Monsoon since marine isotope stage 5.1 (~88 ka). *Climate of the Past*, *10*(5), 1735–1750. https://doi.org/10.5194/cp-10-1735-2014

Thompson, P. R. (1981). Planktonic foraminifera in the western North Pacific during the past 150,000 years: Comparison of modern and fossil assemblages. *Palaeogeography, Palaeoclimatology, Palaeoecology*, *35*, 241–279. https://doi.org/10.1016/0031-0182(81)90099-7

Thompson, P. R., & Shackleton, N. J. (1980). North Pacific palaeoceanography: Late Quaternary coiling variations of planktonic foraminifer Neogloboquadrina pachyderma. *Nature*, *287*(5785), 829–833. https://doi.org/10.1038/287829a0

Ujiié, H., Tanaka, Y., & Ono, T. (1991). Late Quaternary paleoceanographic record from the middle Ryukyu Trench slope, northwest Pacific. *Marine Micropaleontology*, *18*(1–2), 115–128. https://doi.org/10.1016/0377-8398(91)90008-T

Ujiié, Y., Asahi, H., Sagawa, T., & Bassinot, F. (2016). Evolution of the North Pacific Subtropical Gyre during the past 190 kyr through the interaction of the Kuroshio current with the surface and intermediate waters. *Paleoceanography*, *31*(11), 1498–1513. https://doi.org/10.1002/2015PA002914

Vats, N., Mishra, S., Singh, R. K., Gupta, A. K., & Pandey, D. K. (2020). Paleoceanographic changes in the East China Sea during the last ~400 kyr reconstructed using planktic foraminifera. *Global and Planetary Change*, *189*, 103173. https://doi.org/10.1016/j.gloplacha.2020.103173

Vogt-Vincent, N. S., & Mitarai, S. (2020). A persistent Kuroshio in the glacial East China Sea and implications for coral paleobiogeography. *Paleoceanography and Paleoclimatology*, *35*(7). https://doi.org/10.1029/2020PA003902

Wang, L., Li, J., Zhao, J., Wei, H., Hu, B., Dou, Y., et al. (2016). Solar-, Monsoon- and Kuroshio-influenced thermocline depth and sea surface salinity in the southern Okinawa Trough during the past 17,300 years. *Geo-Marine Letters*, *36*(4), 281–291. https://doi.org/10.1007/s00367-016-0448-4

Wang, N., Jiang, D., & Lang, X. (2018). Northern westerlies during the last glacial maximum: Results from CMIP5 simulations. *Journal of Climate*, *31*(3), 1135–1153. https://doi.org/10.1175/JCLI-D-17-0314.1

Wang, Y.-L., & Wu, C.-R. (2018). Discordant multi-decadal trend in the intensity of the Kuroshio along its path during 1993–2013. *Scientific Reports*, *8*(1), 14633. https://doi.org/10.1038/s41598-018-32843-y

Weiss, T. L., Linsley, B. K., & Gordon, A. L. (2021). Pacific North Equatorial current bifurcation latitude and Kuroshio Current shifts since the last glacial maximum inferred from a Sulu Sea thermocline reconstruction. *Quaternary Science Reviews*, *264*, 106999. https://doi.org/10.1016/j.quascirev.2021.106999

Xiang, R., Sun, Y., Li, T., Oppo, D. W., Chen, M., & Zheng, F. (2007). Paleoenvironmental change in the middle Okinawa Trough since the last deglaciation: Evidence from the sedimentation rate and planktonic foraminiferal record. *Palaeogeography, Palaeoclimatology, Palaeoecology*, *243*(3–4), 378–393. https://doi.org/10.1016/j.palaeo.2006.08.016

Xu, X., & Oda, M. (1999). Surface-water evolution of the eastern East China Sea during the last 36,000 years. *Marine Geology*, *156*(1–4), 285–304. https://doi.org/10.1016/S0025-3227(98)00183-2

Yamamoto, M. (2009). Response of mid-latitude North Pacific surface temperatures to orbital forcing and linkage to the East Asian summer monsoon and tropical ocean–atmosphere interactions. *Journal of Quaternary Science*, *24*(8), 836–847. https://doi.org/10.1002/jqs.1255

Yanase, W., & Abe-Ouchi, A. (2010). A numerical study on the atmospheric circulation over the midlatitude North Pacific during the last glacial maximum. *Journal of Climate*, *23*(1), 135–151. https://doi.org/10.1175/2009JCLI3148.1

Yokoyama, Y., Esat, T. M., Thompson, W. G., Thomas, A. L., Webster, J. M., Miyairi, Y., et al. (2018). Rapid glaciation and a two-step sea level plunge into the Last Glacial Maximum. *Nature*, *559*(7715), 603. https://doi.org/10.1038/s41586-018-0335-4

Zhao, J., Li, J., Cai, F., Wei, H., Hu, B., Dou, Y., et al. (2015). Sea surface temperature variation during the last deglaciation in the southern Okinawa Trough: Modulation of high latitude teleconnections and the Kuroshio Current. *Progress in Oceanography*, *138*, 238–248. https://doi.org/10.1016/j.pocean.2015.06.008

Zheng, X., Li, A., Kao, S., Gong, X., Frank, M., Kuhn, G., et al. (2016). Synchronicity of Kuroshio current and climate system variability since the last glacial maximum. *Earth and Planetary Science Letters*, *452*, 247–257. https://doi.org/10.1016/j.epsl.2016.07.028

References From the Supporting Information

Amante, C., & Eakins, B. W. (2009). ETOPO1 1 arc-minute global relief model: Procedures, data sources and analysis. US department of commerce, national oceanic and atmospheric administration, national environmental satellite, data, and information service, national geophysical data center. *Marine Geology and Geophysics Division*, *19*.

Chan, W.-L., Abe-Ouchi, A., & Ohgaito, R. (2011). Simulating the mid-Pliocene climate with the MIROC general circulation model: Experimental design and initial results. *Geoscientific Model Development*, *4*(4), 1035–1049. https://doi.org/10.5194/gmd-4-1035-2011

Hinada, T. (1996). Seasonal variation and long-term trends of the oceanographic conditions along a fixed hydrographic line crossing the Kuroshio in the East China Sea. *Oceanographic Magazine*, *45*, 9–32.

Johns, W. E., Lee, T. N., Zhang, D., Zantopp, R., Liu, C.-T., & Yang, Y. (2001). The Kuroshio east of Taiwan: Moored transport observations from the WOCE PCM-1 Array. *Journal of Physical Oceanography*, *31*(4), 1031–1053. https://doi.org/10.1175/1520-0485(2001)031<1031:TKEOTM>2.0.CO;2

Jordi, A., & Wang, D.-P. (2012). sbPOM: A parallel implementation of Princenton Ocean Model. *Environmental Modelling & Software*, *38*, 59–61. https://doi.org/10.1016/j.envsoft.2012.05.013

Kageyama, M., Merkel, U., Otto-Bliesner, B., Prange, M., Abe-Ouchi, A., Lohmann, G., et al. (2013). Climatic impacts of fresh water hosing under last glacial maximum conditions: A multi-model study. *Climate of the Past*, *9*(2), 935–953. https://doi.org/10.5194/cp-9-935-2013

Locarnini, M. M., Mishonov, A. V., Baranova, O. K., Boyer, T. P., Zweng, M. M., Garcia, H. E., et al. (2019). World Ocean Atlas 2018, volume 1: Temperature. In A. Mishonov (Ed.), NOAA Atlas NESDIS 81 (Vol. 1, p. 52). http://www.nodc.noaa.gov/OC5/indprod.html

Nagano, A., Ichikawa, K., Ichikawa, H., Tomita, H., Tokinaga, H., & Konda, M. (2010). Stable volume and heat transports of the North Pacific subtropical gyre revealed by identifying the Kuroshio in synoptic hydrography south of Japan. *Journal of Geophysical Research*, *115*(C9), C09002. https://doi.org/10.1029/2009JC005747

Ohgaito, R., Sueyoshi, T., Abe-Ouchi, A., Hajima, T., Watanabe, S., Kim, H.-J., et al. (2013). Can an Earth system model simulate better climate change at mid-Holocene than an AOGCM? A comparison study of MIROC-ESM and MIROC3. *Climate of the Past*, *9*(4), 1519–1542. https://doi.org/10.5194/cp-9-1519-2013

O'ishi, R., & Abe-Ouchi, A. (2011). Polar amplification in the mid-Holocene derived from dynamical vegetation change with a GCM: MID-HOLOCENE warming by dynamic vegetation. *Geophysical Research Letters*, *38*(14). https://doi.org/10.1029/2011GL048001

Qiu, B., Nakano, T., Chen, S., & Klein, P. (2017). Submesoscale transition from geostrophic flows to internal waves in the northwestern Pacific upper ocean. *Nature Communications*, *8*, 14055. https://doi.org/10.1038/ncomms14055

Schönau, M., Rudnick, D., Cerovecki, I., Gopalakrishnan, G., Cornuelle, B., McClean, J., & Qiu, B. (2015). The Mindanao current: Mean structure and connectivity. *Oceanography*, *28*(4), 34–45. https://doi.org/10.5670/oceanog.2015.79

Schönau, M. C., & Rudnick, D. L. (2015). Glider observations of the north equatorial current in the western tropical Pacific. *Journal of Geophysical Research: Oceans*, *120*(5), 3586–3605. https://doi.org/10.1002/2014JC010595

Sherriff-Tadano, S., Abe-Ouchi, A., Yoshimori, M., Oka, A., & Chan, W.-L. (2018). Influence of glacial ice sheets on the Atlantic meridional overturning circulation through surface wind change. *Climate Dynamics*, *50*(7–8), 2881–2903. https://doi.org/10.1007/s00382-017-3780-0

Zhang, Z., Qiu, B., Tian, J., Zhao, W., & Huang, X. (2018). Latitude-dependent finescale turbulent shear generations in the Pacific tropical-extratropical upper ocean. *Nature Communications*, *9*(1), 4086. https://doi.org/10.1038/s41467-018-06260-8

Zhu, X.-H., Nakamura, H., Dong, M., Nishina, A., & Yamashiro, T. (2017). Tidal currents and Kuroshio transport variations in the Tokara Strait estimated from ferryboat ADCP data. *Journal of Geophysical Research: Oceans*, *122*(3), 2120–2142. https://doi.org/10.1002/2016JC012329

Zweng, M. M., Reagan, J., Seidov, D., Boyer, T., Locarnini, R., Garcia, H., et al. (2019). World ocean atlas 2018 volume 2. Salinity. World Ocean Atlas 2018 (Vol. 2, p. 50). https://data.nodc.noaa.gov/woa/WOA18/DOC/woa18_vol2.pdf